Proceedings of the 5th International Conference on Civil Engineering for Sustainable Development (ICCESD 2020), 7~9 February 2020, KUET, Khulna, Bangladesh (ISBN-978-984-34-8764-3)

EXPERIMENTAL INVESTIGATION ON MECHANICAL PROPERTIES OF NATURALLY CORRODED STEEL BARS

Matiur Rahman Raju*[1], Amel Cato[2] and Ignasi Fernendez[3]

[1]Senior Lecturer, City University, Bangladesh, e-mail: raju06civil@yahoo.com
[2]Construction Engineer, Sweco, Sweden, e-mail: amel.cato@hotmail.com
[3]Senior Lecturer, Chalmers University of Technology, Sweden, e-mail: ignasi.fernandez@chalmers.se

***Corresponding Author**

ABSTRACT

Corrosion affects reinforced concrete structures in many ways, however, the impact of corrosion in the mechanical properties of the bar itself presents still many uncertainties. The impact of natural corrosion effect and corrosion type in the measured mechanical properties by experimental investigation would be the main objective of this study. The corrosion levels were measured by using different methods such as gravimetric (weight loss) and 3D scanning techniques. Therefore, to perform monotonic tests on steel bars measured by Digital Image Correlation (DIC) techniques were conducted by using different bar diameters and lengths for uncorroded and corroded specimens, with the underlying purpose to investigate the impact of corrosion on the mechanical properties of the steel reinforcement. Further, the post-processing of the results was carried out with the software GOM Correlate Professional. Based on the performed analysis, the 25mm length extensometer was used in combination with the measured force to obtain all the relevant results: strains, displacements, and other important values needed to further acquire engineering stress-strain curves. The obtained results indicate that the mechanical properties of the reinforcing steel bars are strongly affected by corrosion due to loss of cross-sectional area in global and local cases for naturally corroded specimens. Those factors cause degradation of the mechanical properties by increasing corrosion levels.

Keywords: *Steel reinforcement, Digital Image Correlation (DIC), Tensile test, Engineering stress-strain, Critical cross-section.*

1. INTRODUCTION

Despite the used technology at the leading edge and substantial innovations in construction practice and design, corrosion of steel bars in reinforced concrete structures is still considered to be one of the main reasons of deterioration which causes high costs due to repairing and replacing critical corroded elements in reinforced concrete structures (Fernandez, Bairán and Marí, 2016; Tahershamsi et al., 2017). This has directed to rising demand and needs for a better understanding of the structural effects of corrosion. Corrosion of reinforcing steel can be divided into two subcategories: Pitting corrosion and generalized corrosion. Pitting corrosion is characterized by the formation of localized pits along the steel bar when generalized corrosion can be seen as several local pits distributed along the bar. The common outcome for the two subcategories is increased in volume of corrosion products and by so causing the surrounding concrete cover to expand and crack. Furthermore, when a reinforcing steel bar is affected by pitting corrosion and subjected to tension, local effects at the cross-section due to stress concentration and local bending are unveiled. In addition, multi-axial stress behavior is also observed due to the presence of those pits. Hence, due to those mentioned effects, the apparent mechanical properties that state the overall steel bar behavior are affected, producing a performance reduction (Fernandez, Bairán and Marí, 2015, 2016). This leads to a major concern to the structural behavior in serviceability and ultimate limit states, which is investigated in this study.

Many researchers such as U, 2001; Du, Clark and Chan, 2005; Apostolopoulos, 2007; Zhang et al., 2012; Apostolopoulos, Demis and Papadakis, 2013; François, Khan and Dang, 2013; Balestra et al., 2016; Tahershamsi et al., 2017; Zhu et al., 2017; Fernandez, Bairán and Marí, 2016; Fernandez, Bairán and Marí, 2015 have already studied the effects for different corrosion types of steel reinforcement and its influence on the mechanical properties. An experimental study of both natural and artificial corroded specimens for tensile test results showed a significant degradation in ultimate strength. Further studies show that naturally corroded rebars have more affecting mechanical results than artificial corroded rebars (Zhang et al., 2012). Due to the generalized and pitting corrosion of steel reinforcement, the cross-section geometry is changing by the loss of the real cross-section diameter of the specimens (Fernandez, Bairán and Marí, 2016). Many experimental studies were done for artificially corroded rebars than naturally corroded to investigate the impact of corrosion on the mechanical properties of the steel reinforcement. The effects of corrosion on the mechanical properties of reinforcement are critical to understanding the real behavior of naturally corroded reinforced concrete structures is needed. A smaller amount of studies has been conducted to evaluate the mechanical properties of naturally corroded and uncorroded steel bars.

In this current experimental work, the monotonic tests on steel bars measured by Digital Image Correlation (DIC) techniques were conducted to investigate the impact of corrosion degree on the mechanical properties of the steel reinforcement have been identified and discussed.

2. RESEARCH METHODOLOGY

2.1 Test Specimens

In this experimental study, a total of 49 reinforcement test specimens divided into two different sets, organized by the source and characteristics of the bars were tested, see Figure 1. Each group was at the same time divided into two groups to differentiate between corroded and uncorroded specimens. The subtypes are:

- Type A1: 16mm naturally corroded, skewed, reinforcing bars.
- Type A2: 16mm uncorroded, skewed reinforcing bars.
- Type B1: 16mm naturally corroded, straight reinforcing bars.
- Type B2: 16mm uncorroded, straight reinforcing bars.

(a) (b) (c)

Figure 1: Images of some specimens from different sources where figures (a) shows the type A1 and B1 naturally corroded 16mm rebars, (b) shows type A2 uncorroded 16mm rebars, (c) shows type B2 uncorroded 16mm rebars.

2.2 Preparation of Test Specimen

For the experiment purpose, rebars were cut by a horizontal band saw machine with ranging lengths of 300 and 400mm. According to Fernandez et al. (Fernandez, Lundgren and Zandi, 2018), the most common methods to clean the corrosion products of the rebars are metallic brushing, acid immersion and sandblasting. The comparison results of 3D scanning and gravimetric measurements for different cleaning methods shown that the sandblasting cleaning method has the best agreement irrespective of the actual corrosion level. Consequently, after cutting the rebars in specific lengths, the sandblasting cleaning method was used with silica particles to remove all corrosion products from the reinforcing steel in a closed-loop system. After the removal of corrosion products from the corroded specimens, the diameter of the rebars was measured by using the Vernier caliper.

2.3 Corrosion Level Measurements

To be able to draw parallels between the corrosion level and how it is impacting the mechanical properties of the reinforcement steel it is crucial to use accurate and reliable corrosion level measurements. In this study, gravimetric measurements and 3D scanning measurements were used to determine the corrosion level.

2.3.1 Gravimetric Measurements

Gravimetric measurement is a method where the calculations are based on weighted corroded and non-corroded steel reinforcement, i.e. weight loss. This procedure was used because the initial weight of each bar before corrosion was unknown.
When the reference weight of the non-corroded steel reinforcement is established, then the calculation can be performed to check the average corrosion degree by using equation 1. See Table 1 for the calculated corrosion levels for the tested bars.

$$avg.cor.lev = \frac{(n.C. - C.)}{n.C.} \quad (1)$$

where:

n.C is the average weight of the non-corroded reference specimen.

C is the actual corroded specimen weight.

2.3.2 3D Scanning Measurements

The 3D scanning technique method that relies on optical measurements. The 3D-scanned results used in this study are research work conducted at Chalmers University of Technology (Das, unpublished; Berrocal, 2017). For those research works the scanning was performed by using a pair of industrial scaled cameras of five megapixels each, set to film in the stereo setting. A maximum accuracy of 2.0 μm was possible to obtain due to the used cameras, which is sufficient in conditions where the corrosion imperfections on the surface of the reinforcing steel need to be measured. The consequence of the scanning resulted in a fine mesh of surface polygons with triangular shape connected by nodes. For every scanning a number of 2,000,000 to 4,000,000 triangular elements was obtained, creating a high-resolution 3D picture of the scanned specimen detailed enough to gain important information such as: pit distribution, pit depth, pit length and loss of cross-sectional area along the reinforcing steel bar see Figure 2 (Tahershamsi et al., 2017).

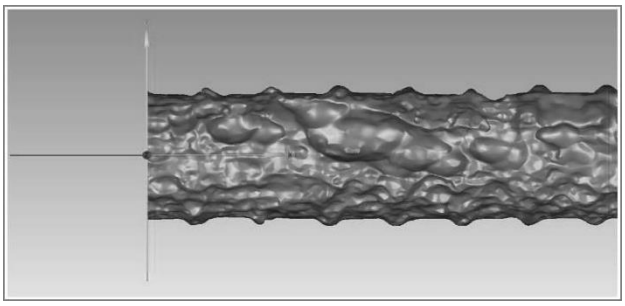

Figure 2: 3D scanned surface of the bar (Tahershamsi et al., 2017)

Based on these two methods the cross-sectional area of the rebar was reduced in two ways: the average (idealized) corroded area along with the rebar, founded on the actual, uncorroded radius and critical cross-section (CCS) reduced area from the 3D scan. The actual (uncorroded), average corroded and CCS areas are respectively displayed in Figure 3. The detailed description of all the acquired parameters is summarized in Table 1.

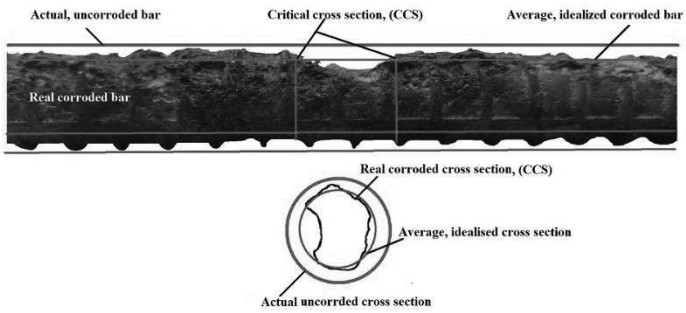

Figure 3: Different type of steel reinforcement areas used in this study

Table 1: Measured specifications of test samples

Type of specimen	Specimen number	Actual diameter [mm]	Average corrosion level (wt. loss) [%]	Average corrosion level (3D scan) [%]	Corrosion at critical cross-section (3D scan) [%]	Actual area [mm^2]	Average (Idealized) area (wt. loss) [mm^2]	Average (Idealized) area (3D scan) [mm^2]	Critical cross-sectional (CCS) area [mm^2]
Type A1	1	16,59	7,5	4,5	13,4	216,05	200	206	187
	3	16,59	8,2	11,4	25,5	216,05	198	191	161
	5	16,59	8,7	7,4	12,3	216,05	197	200	189
	6	16,59	7,2	7,8	21,4	216,05	200	199	170
	8	16,59	7,0	4,0	14,6	216,05	201	207	184
	9	16,59	7,7	8,2	19,3	216,05	199	198	174
	10	16,59	10,1	8,5	12,9	216,05	194	198	188
	11	16,59	8,2	5,9	9,7	216,05	198	203	195
	16	16,59	8,6	7,7	16,7	216,05	197	199	180
	17	-	-		-	-	-	-	-
	18	16,59	7,8	11,5	20,0	216,05	199	191	173
Type A2	U49	16,59	-	-	-	216,05	-	-	-
	U51	16,59	-	-	-	216,05	-	-	-
	U53	16,59	-	-	-	216,05	-	-	-
	U54	16,59	-	-	-	216,05	-	-	-
	U55	16,59	-	-	-	216,05	-	-	-
Type B1	2	16,41	8,0	5,9	11,2	211,60	195	199	188
	4	16,41	9,5	13,5	30,6	211,39	191	183	147
	7	16,41	14,0	10,6	17,8	211,39	182	189	174
	12	16,41	8,7	13,3	26,9	211,39	193	183	155
	13	16,41	5,3	4,3	10,1	211,39	200	202	190
	14	16,41	10,9	12,6	20,0	211,39	188	185	169
	15	16,41	8,9	11,4	16,3	211,39	193	187	177
	19	16,41	8,2	12,5	24,3	211,39	194	185	160
	20	16,41	14,5	16,0	27,1	211,39	181	178	154
	21	16,41	14,2	15,4	19,7	211,39	181	179	170
	22	16,41	5,8	3,4	7,7	211,39	199	204	195
	23	16,41	8,3	8,7	16,7	211,39	194	193	176
	24	16,41	6,1	5,5	17,7	211,39	198	200	174
	25	16,41	7,6	8,2	14,6	211,39	195	194	181
	26	16,41	14,3	15,6	25,0	211,39	181	178	158
	27	16,41	12,8	14,4	18,4	211,39	184	181	173
	28	16,41	7,9	6,6	13,0	211,39	195	197	184
	29	16,41	11,6	10,4	19,1	211,39	187	189	171
	30	16,41	5,8	6,0	13,1	211,39	199	199	184
	31	16,41	4,9	1,7	6,5	211,39	201	208	198
	32	16,41	11,2	9,7	21,8	211,39	188	191	165
	33	16,41	17,8	18,2	30,4	211,39	174	173	147
	34	16,41	5,4	7,6	14,2	211,39	200	195	181
	35	16,41	4,4	3,7	10,3	211,39	202	204	190
	36	16,41	15,4	15,6	20,9	211,39	179	178	167
	37	16,41	15,4	15,4	28,5	211,39	179	179	151
	38	16,41	18,7	25,5	39,0	211,39	172	158	129
	39	16,41	12,3	12,3	20,6	211,39	185	185	168

Type of specimen	Specimen number	Actual diameter [mm]	Average corrosion level (wt. loss) [%]	Average corrosion level (3D scan) [%]	Corrosion at critical cross-section (3D scan) [%]	Actual area [mm^2]	Average (Idealized) area (wt. loss) [mm^2]	Average (Idealized) area (3D scan) [mm^2]	Critical cross-sectional (CCS) area [mm^2]
Type B1	36	16,41	15,4	15,6	20,9	211,39	179	178	167
	37	16,41	15,4	15,4	28,5	211,39	179	179	151
	38	16,41	18,7	25,5	39,0	211,39	172	158	129
	39	16,41	12,3	12,3	20,6	211,39	185	185	168
Type B2	U48	16,41	-	-	-	211,39	-	-	-
	U50	16,41	-	-	-	211,39	-	-	-
	U52	16,41	-	-	-	211,39	-	-	-
	U58	16,41	-	-	-	211,39	-	-	-
	U59	16,41	-	-	-	211,39	-	-	-

2.4 Assessment of Mechanical Properties

After assessing the specifications of the bars, the tensile test to failure was performed on a UTM machine of 250kN capacity with a loading increment of 0.5kN/s. Between the two clamps, the specimen's length was chosen 200mm and the remaining length placed in each clamp for uniform stress distribution. The Digital Image Correlation (DIC) optical non-contact 3D measuring system techniques were used to recorded applied load and elongation with a high-speed camera until the specimen failure. The equipment is, at the same time, connected to a computer responsible for recording the acquired images. The system allows the acquisition of other external data, by connecting it to the optical channels available. In this project, the calibration was set up for measuring areas of 100mm x 20mm following the manufacturer`s guidelines and standards (Wanat, 2016). To use the DIC system a stochastic pattern needs to be applied to the specimen. The post-processing of such measurements allows the obtention of many other relevant parameters. The setup of the DIC system is shown in Figure 4.

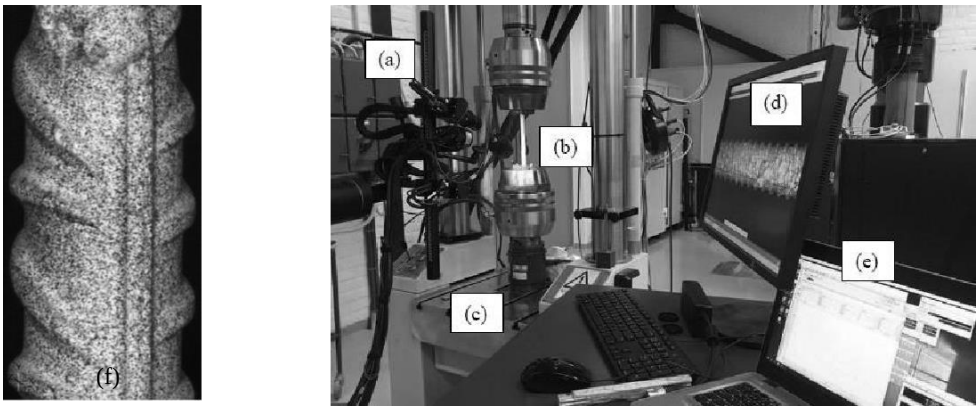

Figure 4: Setup of the Digital Image Correlation (DIC) testing system. (a) double cameras and LED lights, (b) tested specimen, (c) tensile test machine, (d) DIC software, (e) controls for a tensile test machine (f) displays the painted reinforcement bar in a zoomed-in setting displaying the stochastic pattern.

2.5 Post-Processing Analysis Method

In cases of Digital Image Correlation (DIC) method, a tool in the software named "Extensometer" was used to obtain the requested data. GOM tool works in the same manner when compared to physical extensometers. After establishing the function for the GOM extensometer, an analysis of the strain distributions along the measured length was done. For this analysis extensometers length, 25mm was used between the ribs of the reinforcing steel bar. The interference with ribs generates a lot of so-called noise, due to discontinuities in the measurements of the DIC system.

3. RESULTS AND DISCUSSIONS

The experimental results are analyzed and discussed with respect to the influence of corrosion are presented in this section. The main types of graph engineering stress-strain were used extracted and collected different mechanical parameters for the tested rebars.

3.1 Engineering Stress-Strain Correlation

Figure 5 and Figure 6 displays the engineering stress-strain curves for the different type of naturally corroded rebars at various corrosion levels for average and critical cross-section with respect to the uncorroded steel bar. Also considered the increasing corrosion level at a critical cross-section, the stress value is much higher than for average corroded cross-section with increasing corrosion level. The effects of different corrosion levels for different types of bars are analyzed to obtain a correlation between the strengths and corrosion levels. Finally, the behavior of modulus of elasticity with increased corrosion levels is also discussed.

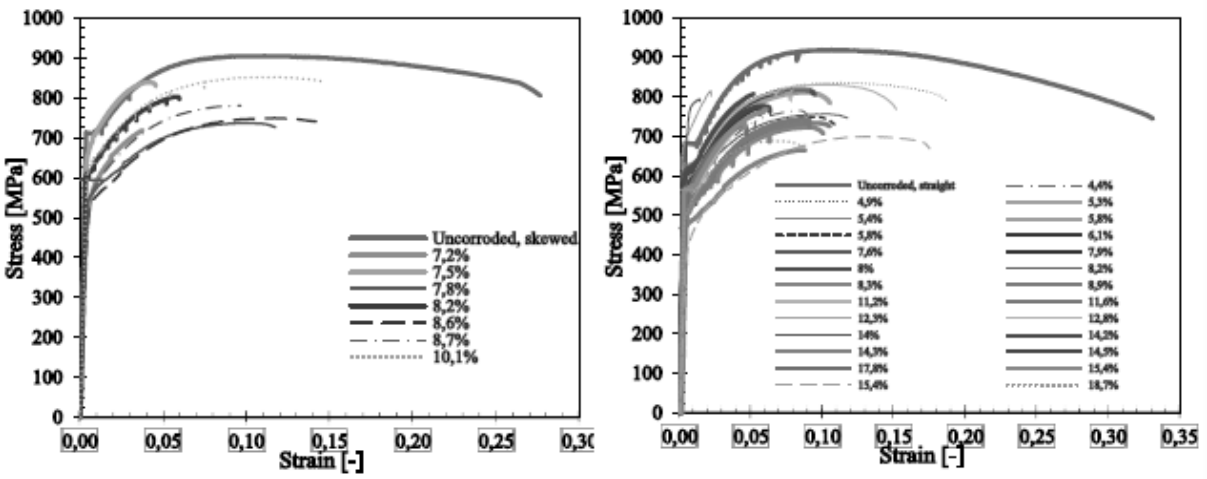

(a) A1 and A2, 16mm skewed bars (b) B1 and B2, 16mm straight bars

Figure 5: Engineering stress-strain curves for a different type of naturally corroded rebars of various corrosion levels at the average cross-section.

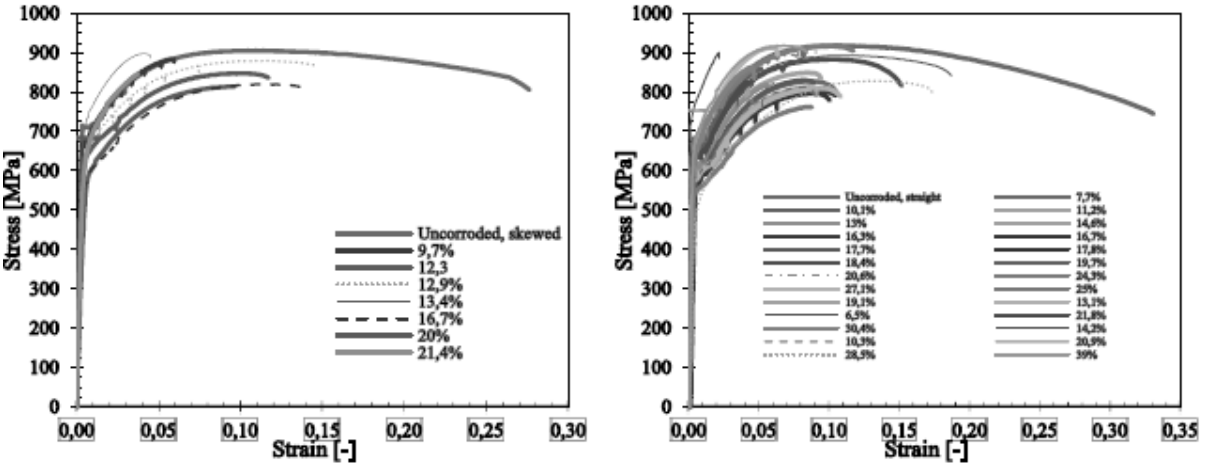

(a) A1 and A2, 16mm skewed bars (b) B1 and B2, 16mm straight bars

Figure 6: Engineering stress-strain curves for a different type of naturally corroded rebars of various corrosion levels at the critical cross-section.

3.1.1 Yield and Ultimate strength

The change of yielding and ultimate strengths depended on increasing corrosion levels which are presented in Figure 7 and Figure 8. The yielding and ultimate strengths produced a reduced trend for considered corrosion levels at the average corrosion level and constant trend for the critical cross-section. For both corrosion levels in Figure 7 and Figure 8, the polynomic fit was used for type (B1, B2) to obtain a high coefficient of correlation, where the linear function was used for type (A1, A2). With this limitation, most of the curves showed that strengths are reducing with increased average corrosion levels. On the other hand, several researchers (Apostolopoulos, 2007; Zhang *et al.*, 2012; Fernandez, Bairán and Marí, 2015) also observed the similar decreasing behavior of yielding and ultimate strengths with increased corrosion levels.

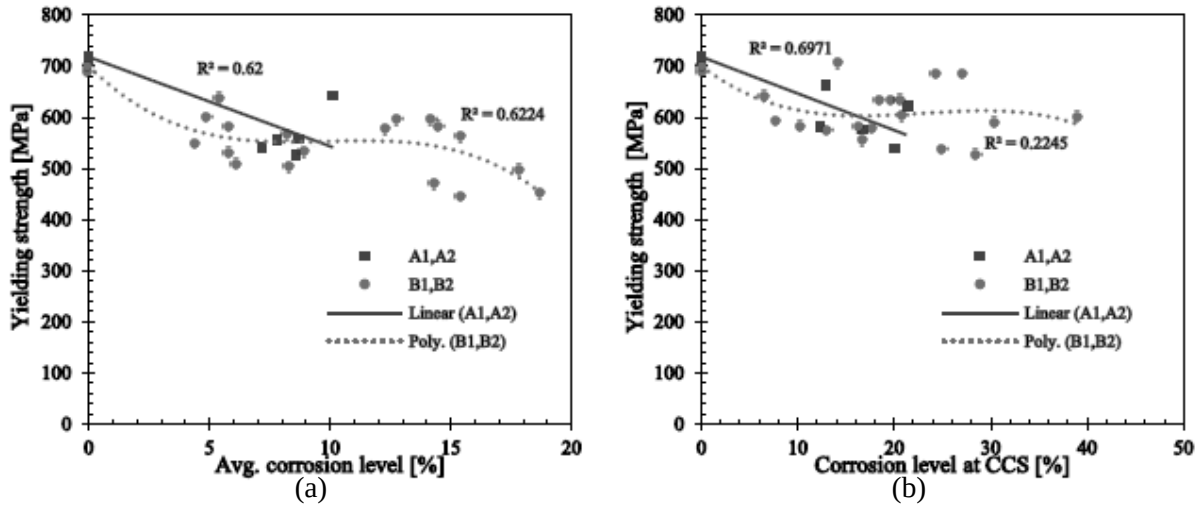

(a) (b)

Figure 7: The yielding strength effect on corrosion levels for a different type of naturally corroded rebars.

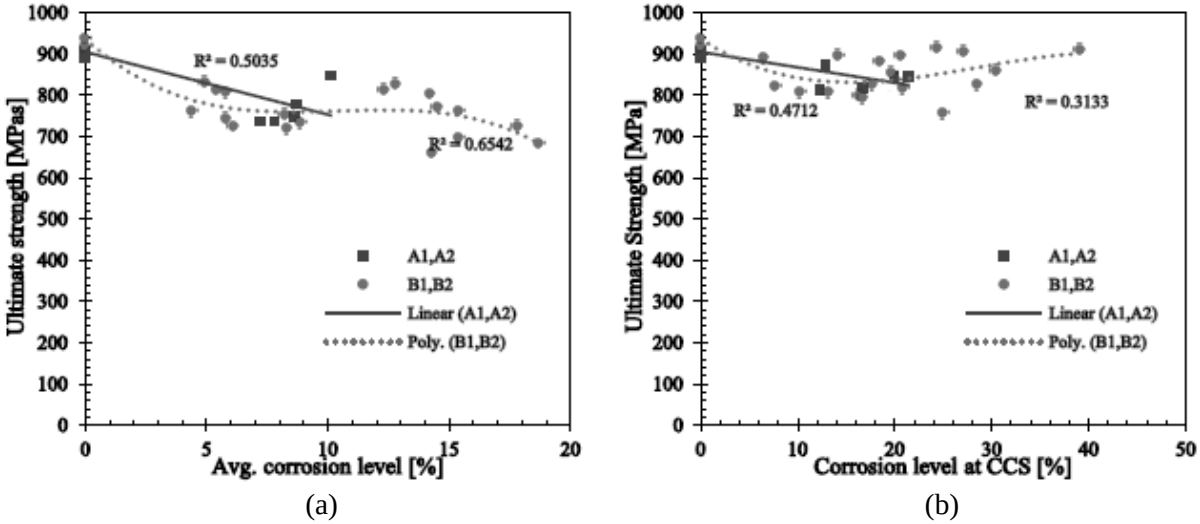

(a) (b)

Figure 8: The ultimate strength effect on corrosion levels for a different type of naturally corroded rebars.

In Figure 7(a) and Figure 8(a) the reducing yield and ultimate strength when considering the average corrosion level. The reduction of the load is higher than the reduction of an area with the increase of corrosion. Due to this difference in reduction, the strength ratio will always be slightly reduced. This reducing behavior was also observed by Llano Trueba, 2015. Further for the CCS section, a reduction

was not noticed as for the average corrosion level, instead, the strength value stayed constant. This can be explained by the CCS method of measuring corrosion level is more realistic and more accurate than average corrosion level, creating a force reduction close to the expected one. The ratio between the force and the area is more or less of the same magnitude and by so resulting in a constant strength value as observed in Figure 7(b) and Figure 8(b).

3.1.2 Modulus of Elasticity

The effect of different corrosion levels on the modulus of elasticity is presented in Figure 9. The modulus of elasticity displayed the highly scatter data disregard of used corrosion type. Because of that, a trustworthy correlation could not be established.

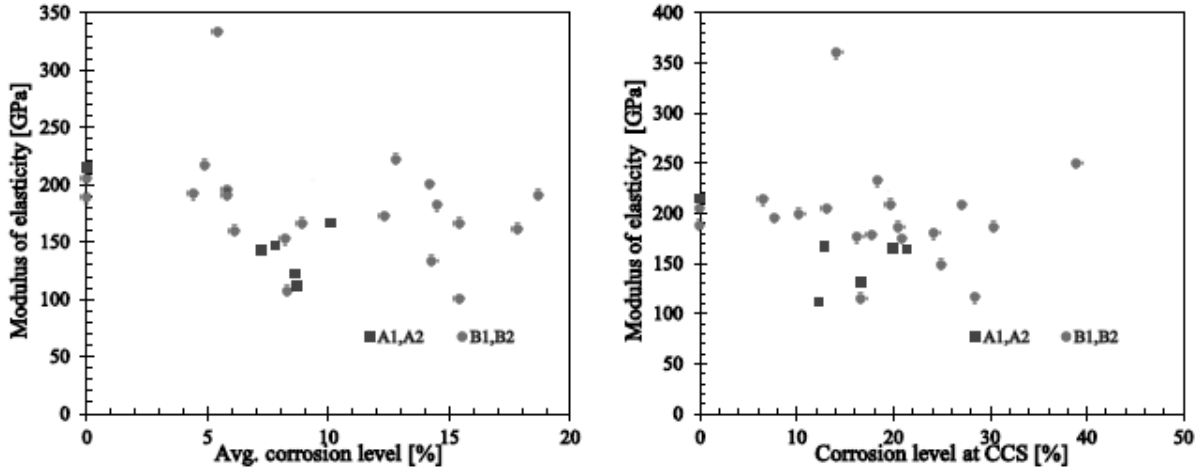

Figure 9: The modulus of elasticity effect on corrosion levels for different type of naturally corroded rebars.

4. CONCLUSIONS

In this study, the average and critical cross-section (CCS) corrosion levels ranged from 0-20% and from 0-40% respectively. However, the observations made for the different parameters were not proportional to the measured corrosion level. The findings presented in this study showed that both the corrosion method i.e. average corrosion and critical corrosion affected the considerate mechanical properties. It can be summarized that method of measuring corrosion in the critical cross was more realistic in its way of describing the behavior. This information will lead to better understanding of the behavior for the reinforced concrete structures and how much they are affected by corrosion.

ACKNOWLEDGMENTS

This research study was undertaken at the Chalmers University of Technology, Division of Structural Engineering and Building Technology, Sweden. We would like to express the sincerest gratitude and appreciation to Ignasi Fernendez, Senior Lecturer, Chalmers University of Technology and his research-team for the support, specifically through hours of meetings, useful advice, expert knowledge, and guideline throughout this study. The authors of the manuscript would like to acknowledge Sebastian Almfeld, a research engineer at the Chalmers University of Technology, for his valuable contribution to the experimental work.

REFERENCES

Apostolopoulos, C. A. (2007) 'Mechanical behavior of corroded reinforcing steel bars S500s tempcore under low cycle fatigue', *Construction and Building Materials*, 21(7), pp. 1447–1456. doi: 10.1016/j.conbuildmat.2006.07.008.

Apostolopoulos, C. A., Demis, S. and Papadakis, V. G. (2013) 'Chloride induced corrosion of steel reinforcement - Mechanical performance andpit depth analysis', *Constr uction and Building Materials*. Elsevier Ltd, 38, pp. 139–146. doi: 10.1016/j.conbuildmat.2012.07.087.

Balestra, C. E. T. *et al.* (2016) 'Corrosion Degree Effect on Nominal and Effective Strengths of Naturally Corroded Reinforcement', *Journal of Materials in Civil Engineering*, 28(10), p. 4016103. doi: 10.1061/(ASCE)MT.1943-5533.0001599.

Berrocal, Carlos G. (2017). 'Corrosion of Steel Bars in Fibre Reinforced Concrete: Corrosion mechanisms and structural performance'. 10.13140/RG.2.2.18233.88166.

Du, Y. G., Clark, L. A. and Chan, A. H. C. (2005) 'Residual capacity of corroded reinforcing bars', *Magazine of Concrete Research*, 57(3), pp. 135–147. doi: 10.1680/macr.2005.57.3.135.

Das, P. (Unpublished) '3D Scanning of naturally corroded steel bars. An assessment of corrosion behavior and correlations to critical cross-sections', Unpublished.

Fernandez, I., Bairán, J. M. and Marí, A. R. (2015) 'Corrosion effects on the mechanical properties of reinforcing steel bars. Fatigue and σ-ε behavior', *Construction and Building Materials*. Elsevier Ltd, 101, pp. 772–783. doi: 10.1016/j.conbuildmat.2015.10.139.

Fernandez, I., Lundgren, K. & Zandi, K. Mater Struct (2018) 51: 78. https://doi.org/10.1617/s11527-018-1206-z

Fernandez, I., Bairán, J. M. and Marí, A. R. (2016) 'Mechanical model to evaluate steel reinforcement corrosion effects on σ-ε and fatigue curves. Experimental calibration and validation', *Engineering Structures*. Elsevier Ltd, 118, pp. 320–333. doi: 10.1016/j.engstruct.2016.03.055.

François, R., Khan, I. and Dang, V. H. (2013) 'Impact of corrosion on mechanical properties of steel embedded in 27-year-old corroded reinforced concrete beams', *Materials and Structures/Materiaux et Constructions*, 46(6), pp. 899–910. doi: 10.1617/s11527-012-9941-z.

Llano Trueba, L. (2015) 'Patterns of corroded rebar surfaces and their impact on tensile mechanical properties.', (August). Available at: http://epubs.surrey.ac.uk/808602/.

Gom.com (2018). *Gom.com*. Retrieved 2018-04-01 from https://www.gom.com/3d-software/gom-system-software/aramis professional.html.

Tahershamsi, M. *et al.* (2017) 'Investigating correlations between crack width, corrosion level and anchorage capacity', *Structure and Infrastructure Engineering*.

U, A. A. A. (2001) 'Effect of degree of corrosion on the properties of reinforcing steel bars', pp. 361–368.

Wanat, S. F. (2016) 'Acquisition : Basic Issues', 25(2), pp. 142–147.

Zhang, W. *et al.* (2012) 'Tensile and fatigue behavior of corroded rebars', *Construction and Building Materials*. Elsevier Ltd, 34, pp. 409–417. doi: 10.1016/j.conbuildmat.2012.02.071.

Zhu, W. *et al.* (2017) 'Influences of corrosion degree and corrosion morphology on the ductility of steel reinforcement', *Construction and Building Materials*. Elsevier Ltd, 148, pp. 297–306. doi: 10.1016/j.conbuildmat.2017.05.079.